

Condition assessment of an 8-year old Freeway bridge, its load capacity and rehabilitation assessment

Ahmad Shayan and Fred Andrews-Phaedonos†*

** ARRB Transport Research, 500 Burwood Highway, Vermont South, Victoria, Australia*

† VicRoads – GeoPave, 12 Lakeside Drive, Burwood East, Victoria, Australia

ABSTRACT

Very early deterioration, in the form of cracking, has started in the in-situ cast concrete columns, cross-heads, abutment and parapet walls, and in the pre-cast, pre-stressed T-beams at the exposed sides of the bridge. The bridge was only 8 years old at the time of the investigation. The vertical cracking of the columns, parallel horizontal cracking of the external faces of the edge T-beams, map-cracking of the cross-head ends, and the abutment walls closely resembled those caused by alkali-aggregate reaction (AAR). However, AAR was not strongly suspected, because it was known that the concrete contains fly ash and due to the relatively early onset of cracking. Representative elements of the bridge were cored and investigated for possible cause(s) of deterioration. The results presented in this paper discount AAR as a cause of cracking at the present time. Three possible mechanisms of distress were identified for this bridge, namely, (a) mechanical overloading causing structural cracking of pier crossheads (and possibly columns); (b) drying shrinkage and (c) cyclic thermal stresses, contributing to the cracking of the columns and external surfaces of the edge beams. The observed cracking, caused by these mechanisms, probably arose from inadequate material formulation, concrete mixing and placement practices. The results of load capacity assessment and recommended rehabilitation are also presented, including carbon fibre strengthening and re-coating with anti-carbonation and finally antigraffiti coatings.

1. INTRODUCTION

The 8-year old Freeway bridge was constructed in 1994 and is a 3-span structure consisting of the following components.

- Case in-situ circular columns and rectangular crossheads;
- Abutments;
- Precast concrete super T-beams. Outer beams cantilevered over the columns with central beams supported by the cantilevered ends;
- Precast parapet units forming the bridge barriers;
- Steel railing.

Recently, cracking has been noted in the columns, crossheads, the outer faces of the exterior beams, the base of the parapet units, and in the abutment walls. The pattern of cracking in the columns and, particularly, the crosshead ends indicated that either alkali-aggregate-reaction (AAR) or shrinkage, or a combination of both may be involved.

The structure was inspected and a few concrete cores were extracted from the columns and a crosshead to investigate the causes of cracking and make recommendations for the

maintenance of the structure. Load capacity assessment was also carried out to ascertain the adequacy of the structure for the current loading and any need for strengthening. This paper presents the results of this investigation.

2. FIELD AND LABORATORY WORK

The following field and laboratory tasks were performed:

- (a) visual assessment and photographic record of the various bridge components.
- (b) extraction of the following concrete core samples (75 mm diameter, 200 mm long), and filling of the core hole with compatible concrete.
 - two cores from a crosshead which exhibited cracking, particularly map-cracking at its ends;
 - two cores from a badly cracked column;
 - two cores from other columns with little or no damage.
- (c) petrographic examination of concrete sampled from each of the elements;
- (d) determination of compressive strength of concrete cores;
- (e) determination of available alkali present in each concrete;
- (f) scanning electron microscopy of concrete from the elements and identification of deleterious reactions involved;
- (g) load capacity assessment and recommendations for rehabilitation.

3. LOCATION OF CORE SAMPLES

Table 1 lists the location of the cores drilled from the various components in Pier 2, and their allocation for the various tests. All the cores were 75 mm in diameter and a cover-meter was used to locate positions that were free of reinforcement bars. The drill holes were filled with Fosroc Rendroc HB40 mortar and coated with primer for better curing.

Table 1: List of cores taken from Pier 2 and tests conducted on them

Element	Condition	Length (mm)	Comp. Strength	Petro-graphy	SEM	Soluble alkali
South Bridge - Column 3	multiple cracks	90 *				
South Bridge - Column 1	1-2 cracks	270	√			
North Bridge - Column 2	single crack	280	√	√		
North Bridge - Column 1	2-3 cracks	270	√		√	√
North Bridge - Crosshead side over Column 1	map cracking and shear cracking	270 §	√	√	√	√
North Bridge - north face of crosshead end	shear cracking	285 §	√		√	

* this core was terminated as it reached a steel bar, which was not cut.

§ these cores are about 1 m apart in the same section of the crosshead of North Bridge.

4. RESULTS

4.1 Visual inspection

A general view of the bridge from the south is shown in Figure 1a, and the close up of Pier 2 which was investigated in this work in Figure 1b. The two end spans are small and are over non-traffic lanes used for maintenance and pedestrian access, the middle span being the largest over all the 8 traffic lanes on both directions. The structure consists of 3 parallel bridges, named “North Bridge”, “Centre Bridge” and “South Bridge”. Figure 2 presents the cross section of the bridge at Pier 2, showing the individual Pier 2 for each of the three bridges, as well as the plan of the crossheads and pile caps at this pier. More details for a typical individual pier are shown in Figure 3. Each pier has three columns numbered 1-3 from left to right. The description of the defects observed in the various components of the bridge are summarised in the following sections.

- ***Precast bridge barrier units (parapet):***

Viewed from the top of the deck, the base of all the parapet units show considerable cracking. The cracking is more extensive in the base of the unit, which is cast in-situ, rather than in the upper part which is precast. Posts at the end of the parapets also show this type of cracking. Typical views are shown in Figure 4. The cracking could have been caused by a single problem, or a combination of problems, including thermal cracking, drying shrinkage, alkali-aggregate-reaction (AAR) and delayed ettringite formation (DEF), but in this case a physical reason may be more likely than AAR and DEF.

- ***Abutments:***

The north and south faces of both abutments consist of 300 mm thick concrete walls, which show considerable random cracking. The north wall of the east abutment has cracks of 0.1–0.2 mm width. These are likely to have been caused by drying shrinkage and/or AAR. The south abutment wall shows more directional cracking rather than map-cracking. Figure 5 shows this type of cracking.

- ***Beams:***

Only the exterior faces of the super T-beams at the two sides of the bridge (north and south) show parallel longitudinal cracking. These could have been caused by the factors mentioned earlier. Figure 6 shows examples of this type of cracking. In one location (east end of the southernmost beam of mid span) faint cracking, which may be due to loading, was noted, as seen in Figure 7. The interior beams appear to be in good condition. However, in some locations on the west abutment side of the Centre Bridge, damage to the beams (braking/cracking), must have occurred due to mishandling during installation or impact by heavy vehicles, and water leakage has occurred through such cracks (Figure 8).

- ***Crossheads:***

Two types of cracking are noted in the crossheads. The exposed ends of the crossheads (i.e. north facing end of the North Bridge crosshead, and south facing end of the South Bridge crosshead) show map cracking that extends into the body of the crosshead. This is very typical of AAR, but could also have arisen from drying-shrinkage (Figure 9). The crossheads in Pier 2 show more obvious cracking than Pier 1. The other type of cracking

appears to be similar to shear-cracking and is evident near the supports in most of the crossheads (Figure 10).

- **Columns:**

Vertical cracking is present in columns of both piers in all the 3 bridges, but it is more extensive towards the southern end of the piers. In some columns there are multiple parallel cracks of 0.2–0.3 mm width (south columns of the South Bridge in both piers), and some other columns exhibit one or two narrower vertical cracks. Examples of these cracks are shown in Figure 11. The cracking in the columns of the Centre Bridge is much less extensive than those shown above.

- **Pile caps:**

The pile caps of Piers 1 and 2 are continuous for all the 3 bridges. The pile cap of Pier 2 is level with the footpath and not visible, but Pier 1 pile cap is raised and shows extensive map-cracking, particularly at the south and north ends (Figure 12). The middle section is relatively free of cracking. This cracking appears very likely to be due to drying-shrinkage, but ARR cannot be discounted. The cracking will increase the carbonation rate of the concrete if it remains untreated. Small roadside walls alongside the pile caps also show similar features (Figure 14).

The visual inspection has detected significant premature deterioration in various components of the bridge. As the cracking (particularly shear-cracking) may indicate deficiencies in the strength of the elements, the affected bridge elements could be considered to be in Fair to Poor condition, although the bridge is only 8 years old.

4.2 Results of laboratory tests

4.2.1 Compressive strength

The results of compressive strength tests conducted on cylindrical samples of 75 mm diameter and 150 mm long are given in Table 2.

Table 2: Compressive strength of cores

Bridge element	Core strength (MPa)	Comments
Column	42.9	The strength specified on the drawings of Pier 2 indicates that the concrete strength grade VR 330 was required for the columns and crossheads. However, based on the strength values, the actual concrete appears to be different for these elements.
Column	48.7	
Column	44.2	
Crosshead side	62.9	
Crosshead end	57.9	

A review of the concrete mix designs in the construction documents indicated that the following mixes (Table 3), were supplied for this structure. The stronger mix for the precast super T-beams is not included here. It is not clear which mixes were used in the different elements.

Table 3: Concrete mixes supplied for the bridge (kg/m³)

Mix type	VicRoads	Pump pave	Pump pave	Special Mix VR400
Nominal slump	80	40	80	80
Cement content [§]	330	385	400	400
Cement type	GB (FA) [§]	GB (FA)	GB (FA)	GB (FA)
Nominal water	—	150	170	170
Water reducer (WRDA) *	300 – 500	300 – 500	300 – 500	300 - 500
Air entrainer *	75	—	—	—
Daracem (l/m ³)	—	1 – 4	—	—
20 mm rhyodacite aggregate	500	530	530	530
14 mm rhyodacite aggregate	200	530	530	530
10 mm rhyodacite aggregate	305	—	—	—
Montrose minus 5 mm	—	100	100	100
Sand 1 minus 5 mm	100	—	—	—
Sand 2	755	665	655	655
Concrete grade (F _c , MPa)	32	40	40	40

[§] = the binder contained 15% fly ash

* = ml/100 kg cement

The target strength (28-days) of the “VicRoads” mix is about 80% of the strength achieved by columns (Table 2), and indicates that this mix was used for the columns. The target strength of the other mixes is 66% of the strength achieved by the crosshead, and indicates that a stronger concrete was probably used than that specified.

4.3 Petrographic examination

Large petrographic thin sections were prepared from some cores for petrographic examination, and the results are described below.

Column 3, South Bridge

The coarse aggregate is composed predominately of a fine-grained acid volcanic origin (rhyodacite), consisting of a mixture of microcrystalline quartz and feldspar with a considerable amount of opaque minerals of fine to medium grain size. Some particles are very uniform, and some others exhibit various degrees of fine veinlet formation. Some of the veinlets include altered feldspar grains in their enlarged portions, around which, and into the veinlets, calcium carbonate formation is observed. In some aggregate particles this feature is seen around feldspar phenocrysts in the rock matrix.

Occasional aggregate particles show a high degree of weathering and iron-oxide formation, and some veinlets appear to contain fine micaceous materials. Some other particles appear to be of a tuffaceous nature, including relatively large (1 – 3 mm) crystal fragments in a very fine-grained siliceous matrix. The latter type has the same abundance as the uniformly textured particles. Some particles contained areas exhibiting typical chalcedonic features. Some degree of orientation was evident in most particles, although those with a uniform texture showed a far lesser degree of orientation. Some crystals included in the tuffaceous particles show considerable iron-oxide formation, indicating their weathered nature.

The fine-grained siliceous nature of the coarse aggregate indicates that it may be susceptible to alkali-aggregate-reaction (AAR). The fine aggregate fraction consists of a natural sand with rounded particles of quartz and feldspar. They are largely monomineralic and monocrystalline but some polycrystalline particles are also present. The majority of quartz grains are stress-free or with a small degree of strain, and occasional particles of moderately-strained quartz are also present. The sand component is probably not sensitive to AAR.

The hydrated cement phase is largely free of microcracking, and appears under plane polarised light to contain a considerable amount of opaque cement minerals, probably calcium-ferro-aluminate. Fine brown particles, probably originating from the aggregate phase are scattered throughout the paste phase.

Column 2, North Bridge

The coarse aggregate in this section is essentially the same as that described above, but the proportion of the tuffaceous particles is greater than that of the uniform particles. Also much stronger evidence of orientation and flow is evident in these particles. In addition, occasional particles showed strong chloritisation in some portions of the aggregate. The sand fraction and the cementitious phase are the same as those in the thin section from Column 3.

Crosshead

The coarse aggregate is similar to that described for column 2 above. The aggregate distribution is different from those in the other sections in that the size of particles is somewhat smaller, and the proportion of the coarse aggregate appears to be larger in this section. This is consistent with the mix proportions for columns and crossheads (Table 3). The sand fraction and the paste phases are also the same as in the other two samples.

No indication of AAR was detected in the sections examined from the various elements.

4.4 Scanning electron microscopy (SEM) and Energy-dispersive x-ray (EDX) analysis

The purpose of the SEM examination was to detect and identify any chemical reaction, such as AAR or DEF, that could have contributed to the observed cracking. It should be noted that the 8-year old bridge is too young to have developed sufficient amounts of AAR products to be diagnosed by unaided eye. It should also be noted that significant AAR expansion and cracking could develop at the stage of aggregate expansion, before reaction products become widespread in the concrete. It could be very difficult to diagnose the presence of AAR in the concrete at this early stage. Nevertheless, it was decided that the SEM and EDX examinations would be the most powerful methods for the diagnosis.

Specimens from the more extensively cracked columns 1 and 3 of the South bridge and specimens from the moderately cracked crosshead of the North bridge were selected for the SEM examinations.

The surfaces of the aggregate particles were either clean fractures, or had thin adhering cement paste. On no occasion were the aggregate particles associated with AAR products, which have distinct morphological features and compositions.

The hydrated cement phase was found to be enriched in Si and Al, compared to the usual calcium-silicate hydrate (CSH) produced as a result of hydration of ordinary Portland cement. This was very likely due to the incorporation of fly ash in the concrete, and Figure 13 shows the composition of the paste in the vicinity of two sites of reacted fly ash particles (round

features to the right). More significant enrichment of the paste with Si and Al are seen in Figures 14 and 15. Although the aggregate exhibited petrographic features of a reactive aggregate, the incorporation of fly ash appears to have prevented the occurrence of AAR. Moreover, the composition of the cement paste indicate very little alkali to be present, and this may be another reason why the aggregate has not exhibited signs of AAR. (As mentioned earlier, it would be too early for this to have happened on a large scale).

Porous areas were observed in some locations (Figure 16), in which the cement paste was also enriched in Si, but crystals of ettringite had also grown in the open spaces. This may have occurred due to localised high water/cement ratios in these regions.

In summary, the SEM and EDX examinations could not provide direct evidence of any deleterious chemical reaction (such as AAR and DEF) as the cause of the observed cracking. The probability that physical mechanisms such as drying-shrinkage have been involved in the cracking is strengthened. Of course, some of the characteristic shear-cracking are probably due to excessive traffic loading.

If the cracking is due to shrinkage, then it would stabilise soon and repair could then be performed. If AAR develops, then the ongoing expansion would need to be controlled, probably by mechanical means. Those cracks which are due to traffic loading indicate that strengthening of the affected elements may be required.

4.5 Alkali content of concrete

The soluble alkali content of the selected concrete samples was determined on powdered specimens of < 150 µm particle size. The results are given in Table 4.

Table 4: Soluble alkali content of concrete

Location	Alkali content kg/m ³		
	Na ₂ O	K ₂ O	Na ₂ O equiv. *
Column 3 – South Bridge	1.23	1.77	2.40
Column 1 – North Bridge	1.47	1.81	2.66
Crosshead – North Bridge	1.05	2.67	2.80

* Na₂O equiv = % Na₂O + 0.658 (% K₂O)

The amount of soluble alkali extracted from the specimens ranges between 2.40–2.80 kg/m³, including the amount released from the aggregate phase, which may amount to 0.5 kg/m³ for the aggregate involved. The corrected alkali content of about 2.0–2.3 kg/m³ would translate to a cement Na₂O equivalent of 0.50–0.60%, which is considered to be a low alkali content in the cement. This level of alkali would not cause serious AAR, unless a considerable amount of alkali is released from the aggregate. On the other hand, if the reactive components in the aggregate have already absorbed some alkali, then the residual amounts extracted may be sufficient to sustain a low-moderate reaction. Future observations and sampling in 5 years time may shed light on this aspect.

5. STRUCTURAL ANALYSIS

The load capacity of the structural elements in the bridge was determined against T-44 and SM1600 live loads and the relevant dead loads. For the super T-beams, the load capacity was

found to be adequate, and the observed cracking at the exterior faces of the edge beams could not be explained by insufficient load capacity. The columns were also found to have sufficient load capacity but they are currently experiencing stresses up to 80% of their load capacity, indicating that the parallel vertical cracking is probably unrelated to mechanical loading. It would be better to improve the load capacity of the columns such that current loading does not exceed 60% of the load capacity.

The crossheads, however, were found to have insufficient load capacity against T-44 and SM1600 loading, requiring an additional 33% tensile steel for the cantilever to resist the bending moment. The mid-span would require 16.6% more steel reinforcement at the top compared to the current configuration. The observed structural cracking of the crossheads could be explained by insufficient load capacity. It appears that other factors have contributed to the development of non-structural cracking in the crosshead ends, and to the cracking of columns and the edge beams.

6. THERMAL STRESS ANALYSIS

Finite element modelling was used to determine thermal stress distribution in the various elements and whether the observed cracking could be related to this factor. For the super T-beams, it was suspected that solar radiation on the exterior surfaces of the edge beams and possibly rapid cooling, as a result of a change in weather, could create large thermal gradients associated with cracking. Similar considerations were given to the cracking of columns and crossheads. Although the finite element model showed that considerable thermal stresses could be generated in these elements due to thermal effects, these stresses were not large enough to cause cracking in one cycle. These results indicate that thermal cycling and very probably drying shrinkage of concrete combined to contribute to the cracking which could not be explained by the structural analysis.

Among the various concrete elements, the crossheads exhibit the influence of all these factors, whereas the exterior faces of the edge beams, the columns, pile caps, the abutment walls and the precast parapet units largely reflect the influences of thermal cycling and drying shrinkage. At the current age, harmful chemical reactions do not appear to have played a role.

7. CONCLUSIONS

Field inspection of the various components of the Freeway bridge has detected considerable cracking in some elements. Despite the presence of a potentially reactive aggregate, deleterious chemical reactions such as AAR and DEF do not appear to have caused the cracking at the current young age (8 years) of the structure. This is probably due to the use of low alkali cement and fly ash in the concrete. Structural analysis showed adequate load capacity for beams and columns, but significant deficiencies for the crossheads, which explains the structural cracking of the latter elements. Thermal stresses and restrained drying-shrinkage could have been the main reasons for the cracking of the other elements. Possibly, the use of extra water in the casting of the elements, additional to that of the prescribed mix design, during casting of the elements augmented the drying shrinkage. Poor curing may also have played a role. The observed cracks need to be repaired to prevent further deterioration of the elements. The structural cracking in the crossheads are related to traffic loading and strengthening of the elements is required immediately.

8. RECOMMENDATIONS

Considering the results of this investigation, the following recommendations are made:

1. Strengthening of the crossheads particularly in the cantilever section by either of steel plating, carbon fibre composite system, installation of additional supports or external post-tensioning.
2. Repair vertical cracks in columns and map cracking in crossheads by epoxy injection and maintain the existing surface coating of all the elements.
3. Repair shrinkage cracks in abutment walls and Pier 1 pile cap by epoxy injection and application of an anti-carbonation coating.
4. Examine concrete core samples from the precast T-beams and barrier units and verify the cause of cracking of the exterior faces of the edge beams and of the precast barrier units, and treat them accordingly.
5. Undertake sampling and testing of substructure for AAR in 5 years time.

A preliminary assessment indicated that the repair and strengthening of the bridge would cost approximately \$400,000.

9. ACKNOWLEDGEMENT

The authors thank VicRoads for funding this work and permission to publish. The opinions expressed in this paper are those of the authors and not necessarily of their respective organisations.



Figure 1a: General view of bridge from the south. Melbourne CBD is to the left.



Figure 1b: Pier 2 from which cores were taken, viewed from the North.

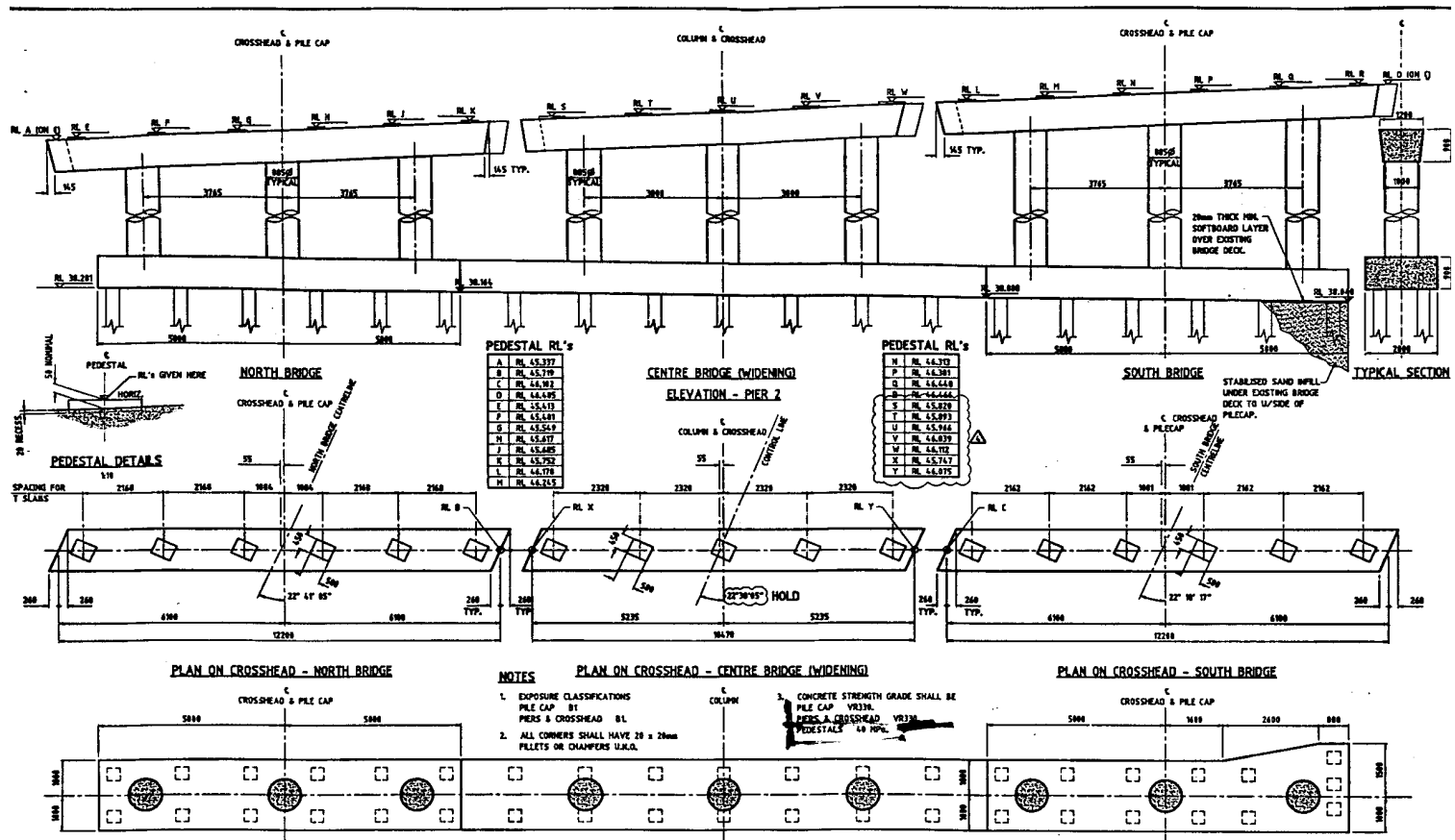


Figure 2: Cross section of structure at Pier 2, showing individual piers for North (left), Centre and South (right) bridges

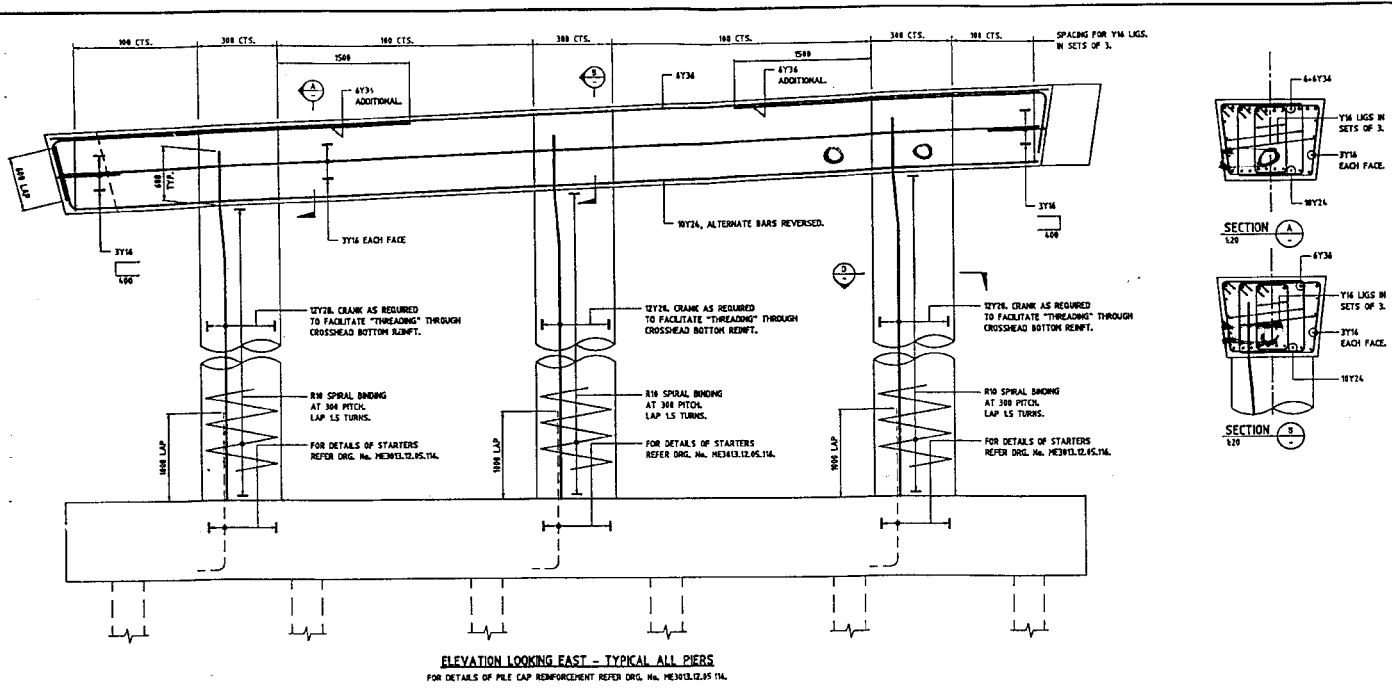


Figure 3: Typical Pier configuration



Figure 4: Cracking in the base of the parapet unit (4A) and in a post (4B).



Figure 5: Cracking in the north wall of the east abutment.



Figure 6: Longitudinal parallel cracking on the exterior face of the southern-most beam of the middle span.



Figure 7: Weak radial cracking at the lower corner of the left beam (southernmost beam, middle span).



Figure 8: Cracking in the flange of some super T-Beams at the left abutment, probably resulting from mishandling or impact by heavy vehicles.



Figure 9: Map-cracking at the south end of the south bridge crosshead. Cracking extends into the element.



Figure 10: Close up of a shear crack in the crosshead.



Figure 11: Multiple parallel vertical cracking in the southern-most column of Pier 2.



Figure 12: Map-cracking in the north end of pile cap of Pier 1, probably due to drying-shrinkage.

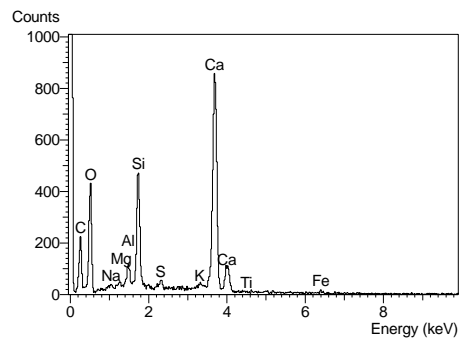
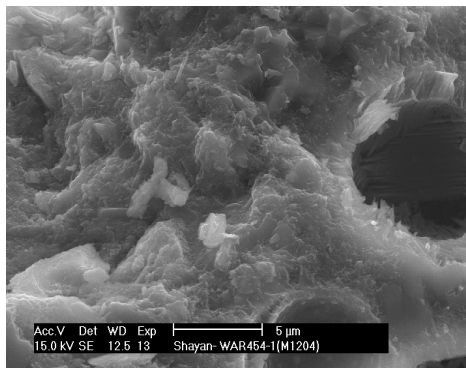


Figure 13: View of hydrated cement paste and its composition represented by the EDX spectrum

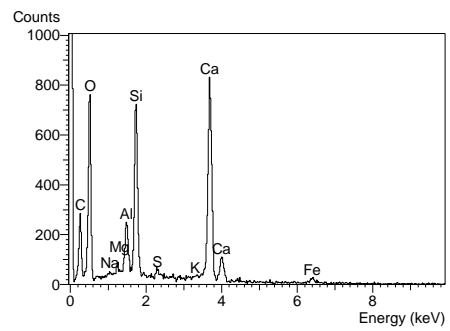
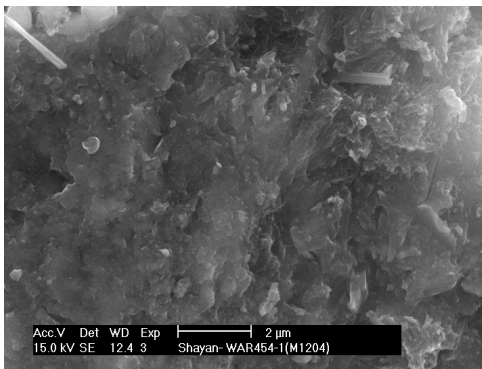


Figure 14: SEM view of paste enriched with Si from fly ash and its EDX spectrum

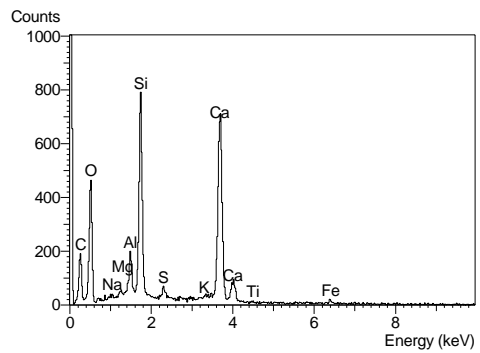
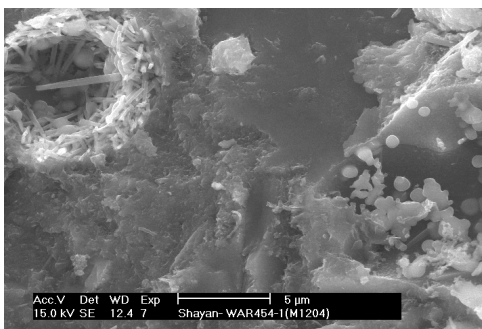


Figure 15: SEM view of another area showing enrichment with Si, and its EDX spectrum

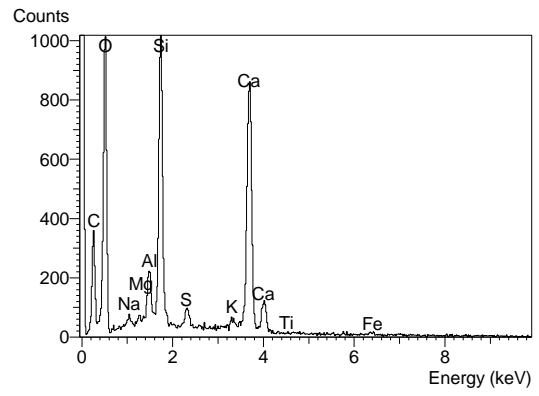
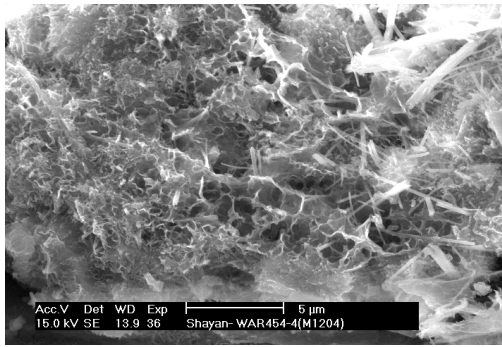


Figure 16: Porous area in cement paste probably indicating zone of high water content. The paste is enriched in Si.